

A SEARCH FOR STABLE PARTICLES HEAVIER THAN THE PROTON

AND FOR $Q = -2/3$ QUARKS PRODUCED IN e^+e^- ANNIHILATION*

J. M. Weiss, G. S. Abrams, M. S. Alam,[†] C. A. Blocker, A. Blondel, A. M. Boyarski, M. Breidenbach, D. L. Burke, W. C. Carithers, W. Chinowsky, M. W. Coles,^{††} S. Cooper,^{††} W. E. Dieterle, J. B. Dillon, J. Dorenbosch,[‡] J. M. Dorfan, M. W. Eaton, G. J. Feldman, M. E. B. Franklin, G. Gidal, G. Goldhaber, G. Hanson, K. G. Hayes,[‡] T. Himel,[‡] D. G. Hitlin,^{‡‡} R. J. Hollebeek, W. R. Innes, J. A. Jaros, P. Jenni,[‡] A. D. Johnson, J. A. Kadyk, A. J. Lankford, R. R. Larsen, M. Levi, V. Lüth, R. E. Millikan, M. E. Nelson, C. Y. Pang, J. F. Patrick, M. L. Perl, B. Richter, A. Roussarie, D. L. Scharre, R. H. Schindler,[‡] R. F. Schwitters,[#] J. L. Siegrist, J. Strait, H. Taureg,[‡] M. Tonutti,^{##} G. H. Trilling, E. N. Vella, R. A. Vidal, I. Videau,[§] and H. Zaccone.[¶]

Stanford Linear Accelerator Center
Stanford University, Stanford, CA 94305
and

Lawrence Berkeley Laboratory and Department of Physics
University of California, Berkeley, CA 94720

ABSTRACT

We have searched 1.4×10^6 e^+e^- annihilation events for particles with $1-3 \text{ GeV}/c^2$ mass and charge $Q = -2/3$ from the processes $e^+e^- \rightarrow q\bar{q}X$ and $e^+e^- \rightarrow q\bar{q}$. Upper limits of $R_Q \sim 10^{-4}$ for each process are presented which improve the previous limits on free quark production in electromagnetic interactions by 2 orders of magnitude.

Submitted to Physics Letters B

* This work was supported primarily by the Department of Energy under contracts DE-AC03-76SF00515 and W-7405-ENG-48.

Present addresses:

[†] Vanderbilt University, Nashville, TN 37235.

^{††} DESY, Hamburg, Fed. Rep. of Germany.

[‡] EP Division, CERN, Geneva, Switzerland.

^{‡‡} California Institute of Technology, Pasadena, CA 91125.

[#] Harvard University, Cambridge, MA 02138

^{##} Universität Bonn, Fed. Rep. of Germany.

[¶] CEN-Saclay, France.

[§] LPNHE, Ecole Polytechnique, Palaiseau, France.

The possible observation of free quarks [1] at the level of 10^{-20} $(q+\bar{q})/\text{nucleon}$ in niobium has given new incentive to the search for fractionally charged particles using accelerators. Although it would seem reasonable to look in processes where quarks are believed to be directly produced, such as deep inelastic scattering and e^+e^- annihilation, the fact is that free quark searches using electromagnetic interactions are few in number and not severely constraining [2-6]. Most past searches have looked for pair production of quarks on nuclear targets using bremsstrahlung photons from high energy electron beams. Their measured limits can be described in terms of the ratio R_Q of the quark production cross section to the cross section for point-like QED particles of the same charge and mass. The most sensitive of these results are from Galik et al. [5] and, for charge $Q = 2/3$ quarks and R_Q assumed to be 1.0, these place a lower limit on mass m_Q of $1.8 \text{ GeV}/c^2$. Better limits have recently been obtained in e^+e^- annihilation at PETRA using the JADE-jet chamber [6]. For quark masses up to $12 \text{ GeV}/c^2$ and $Q = 2/3$, they place 90% C.L. upper limits on R_Q of the order of 10^{-2} . This letter presents results which are yet 2 orders of magnitude more sensitive in R_Q for $Q = 2/3$ quarks in the range of m_Q between 1 and $3 \text{ GeV}/c^2$.

We have undertaken a search for $Q = -2/3$ and $Q = -1$ particles with mass greater than a proton mass in e^+e^- annihilation using the SLAC-LBL Mark II detector at the SPEAR e^+e^- storage ring of the Stanford Linear Accelerator Center. We have conducted high statistics searches in two general categories of events. The first search is for inclusive quark production from the process $e^+e^- \rightarrow q\bar{q}X$ in a sample of 9.8×10^5 multi-prong and non-coplanar 2-prong events. These events contain 2.7×10^6

observed tracks in the detector from a total integrated luminosity of 19900 nb^{-1} which represents all of the Mark II data taking at SPEAR with c.m. energies between 3.9 and 7.4 GeV. The second search uses a sample of 7.7×10^5 tracks from 3.85×10^5 colinear 2-prong events in the same energy range to search for the process $e^+e^- \rightarrow q\bar{q}$.

Detailed descriptions of the detector have been given elsewhere [7-9]. The trigger for this experiment requires one track to register in the drift chambers and the appropriate one of 48 time-of-flight scintillation counters (0.75 of 4π solid angle) as well as a second track to register in the inner layers of the drift chamber. Our understanding of the drift chamber implies highly relativistic particles with $Q = 2/3$ should provide more than sufficient primary ionization to keep the drift chamber tracking fully efficient. Furthermore, as will be shown, massive $Q = 2/3$ quarks produced in colliding beams at SPEAR energies are expected to be so slow as to actually leave substantially more than minimum ionization. The thresholds for the time-of-flight counters are sufficiently low to be fully efficient for highly relativistic $Q = 2/3$ particles and this is empirically verified by reducing the light output of the N_2 flashlamp/silica optical fiber system used to continually align and calibrate the time-of-flight system. In order to reach the time-of-flight counters, particles must traverse at least 2.6 g/cm^2 of carbon, or equivalent, and 1.7 g/cm^2 of aluminum.

The first search, for $e^+e^- \rightarrow q\bar{q}X$, uses the time-of-flight system to measure the velocity, $\beta = v/c$, of all tracks. The average timing resolution for hadron tracks is $\sigma = 0.30$ nsec over flight-times which are

5-7 nsec for $\beta = 1$ particles but up to 45 nsec for particles with masses of interest here. Reconstructed tracks are required to be aimed toward the time-of-flight system (92%), to be 2 cm away from a counter edge and 5 cm away from a counter end (80%). The counter must be intersected by only 1 reconstructed track (96%). Further, the z position along the counter can be determined from the time difference of the signals from the XP2230 phototubes viewing each end and this must agree to ± 25 cm with the z position from the particle trajectory (98%). A final requirement is made that the particle trajectory pass through all 16 layers of the drift chamber (96%). The percentages given here represent the efficiencies for each cut as measured with low mass particles.

Combining the time measurement with the apparent momentum, $p = p_Q/Q$, the detector determines a mass

$$m_T^2 = \frac{p_Q^2}{Q^2} (1/\beta^2 - 1) = \frac{m_Q^2}{Q^2} .$$

Figures 1a and 1b show the observed spectrum of time-of-flight masses m_T^2 for $Q > 0$ and $Q < 0$, respectively, for all tracks with $m_T^2 > 1.6 (\text{GeV}/c^2)^2$, (4482 tracks). Here p, β and thus m_T^2 have been corrected for energy loss through the detector of $Q = 1$ particles. Also indicated in fig. 1a are the expected locations of deuterons and tritons. Although their absence from the negatively charged data of fig. 1b implicates beam-gas collisions as the source of these particles, they illuminate our acceptance and provide excellent calibration signals which can be used to study the response of the detector to massive stable particles. The negatively charged data are relatively uncontaminated by beam-gas events and can be searched for new massive particles.

Fits to the $Q = +1$ data of fig. 1a give masses $1.89 \pm .01 \text{ GeV}/c^2$ and $2.83 \pm .07 \text{ GeV}/c^2$ and widths $\sigma_{m_T}^2$ of $.45$ and $.86 (\text{GeV}/c^2)^2$ for the deuteron and triton signals, respectively. Fixing these masses and widths, one can then fit the $Q = -1$ data of fig. 1b and arrive at upper limits on the number of events from inclusive \bar{d} and \bar{t} production in e^+e^- annihilation. These limits are $N(\bar{d}) \leq 9.3$ events and $N(\bar{t}) \leq 9.0$ events at the 90% confidence level. Efficiencies of 47% and 46%, respectively, are calculated using a hadronic production model $E(d^3\sigma/dp^3) \propto e^{-bE}$ with $b(E_{c.m.}) = 4.9-4.2 \text{ GeV}^{-1}$ which well describes all other hadron production in this energy range [9]. For integrated luminosities above threshold of 19891 nb^{-1} and 5178 nb^{-1} , respectively, these limits correspond to cross sections less than 1.0 pb and 3.9 pb for \bar{d} and \bar{t} production. These cross section limits then also hold approximately for any other massive stable particle, q , with charge $Q = -1$ and ordinary nuclear interactions. Using the average c.m. energies above threshold of 5.3 and 6.7 GeV , respectively, they can be expressed as limits on R_Q which we define as the ratio of the production cross section to the μ -pair cross section

$$R_Q = \frac{\sigma(e^+e^- \rightarrow q\bar{q}X)}{\sigma(e^+e^- \rightarrow \mu^+\mu^-)}$$

These limits then become $R_Q \leq 3.1 \times 10^{-4}$ for the surrounding mass region $m_Q = 1.7 - 2.3 \text{ GeV}/c^2$ and $R_Q \leq 1.9 \times 10^{-3}$ for $m_Q = 2.3 - 3.0 \text{ GeV}/c^2$ for $Q = -1$ at the 90% confidence level.

To search for particles with charge $Q = 2/3$, the pulse height measurement can be used to obtain information on the ionization loss of

each track. After correction for particle pathlength, light attenuation in the 2.54 cm Pilot F scintillator and electronics nonlinearities, one obtains the dE/dx distribution shown in fig. 2a for all tracks with $m_T^2 > 1.6 \text{ (GeV/c}^2\text{)}^2$. The calibration is fixed by the average pulse height recorded for μ pairs and Bhabha scattered electrons in each counter. It is apparent that, in contrast to the positively charged data, the negatively charged tracks in fig. 2a overwhelmingly have dE/dx values which are consistent with those of minimum ionizing $|Q| = 1$ tracks [10], rather than strongly ionizing, low β massive tracks. As we are looking for weakly ionizing $Q = -2/3$ massive tracks, we have also plotted in fig. 2b the ratio of the measured dE/dx to the most probable energy loss calculated [11 - 14] for $|Q| = 1$ and for β corrected to the entrance of the scintillator. To better than 15% this ratio is equal to the charge squared Q^2 of the particle. The width of the $Q > 0$ distribution in fig. 2b represents an energy loss resolution of $\sigma = 20\%$.

The dashed curve in fig. 2b shows the expected distribution for $Q = -2/3$, scaled from the measured deuterons and tritons. If we impose a cut on $dE/dx / (dE/dx)_{\text{pred}}$ which is between 20% and 65% of the value expected for $|Q| = 1$ particles, we should remain fully efficient for $Q = -2/3$ tracks.

Figure 3 then presents the same data as fig. 1b but after applying the dE/dx cut described above and with energy loss corrections to p and β performed according to $Q = -2/3$. In addition, a vertex requirement has been imposed on the measured tracks which is fully efficient for primary particles from beam-beam collisions, but which reduces background contributions from beam-gas and other interactions. The data

are presented in Fig. 3 as a scatter plot of apparent momentum versus $m_T^2 = m_Q^2 / Q^2$. Regions which could be populated by typical quark masses of $m_Q = 1.25$ and $2.3 \text{ GeV}/c^2$ are indicated. In our search, such regions are determined for each value of m_Q by the $\pm 2\sigma$ contours of the calculated m_T^2 resolution, the maximum momentum allowed by kinematics and the minimum momentum due to range cut-off for $Q = 2/3$. The m_T^2 resolution calculation has been verified in detail for all detected particles.

Table I then presents the maximum number of events observed for quark masses in each of several quark mass intervals and the 90% confidence level upper limits based on those events. For higher masses ($m_Q > 1.9 \text{ GeV}/c^2$), these limits are based simply on the total number of events observed within the contour region corresponding to each value of m_Q . However for lower masses, ($1.0 - 1.9 \text{ GeV}/c^2$), a background subtraction has been performed using sidebands given by the $\pm 2\sigma$ and $\pm 4\sigma$ contours for each m_Q . To minimize efficiency corrections for events which could be lost due to the effects of increased m_T^2 resolution at the highest momenta, luminosity used for $m_Q = 1.0$ to $1.25 \text{ GeV}/c^2$ was limited to that from 5.2 GeV and below.

Table I then translates these event limits into limits on cross section and on R_Q . Quarks are assumed here to undergo normal nuclear interactions, i.e., a quark nuclear cross section of 10 mb/nucleon which gives a 3% loss per track. The efficiency calculation uses the hadronic production model described previously but the search technique used here makes the efficiencies extremely model independent.

The second search is for $e^+e^- \rightarrow q\bar{q}$ in the colinear 2-prong data sample which is dominated by μ -pair and Bhabha scattering events.

Here we require colinearity less than 10^0 and that the apparent momentum, p_Q/Q , is greater than $\frac{1}{2}$ the beam energy, E_b . This momentum cut imposes a minor restriction on quark mass of $m_Q < .94E_b$ for $Q = 2/3$. If we then impose on both tracks the same cut on $dE/dx / (dE/dx)_{\text{pred}}$ that was applied to tracks in the previous inclusive analysis, no event candidates remain with both $m_T^2 > 1.0 \text{ (GeV/c}^2\text{)}^2$. Table II then shows the calculated efficiency for a $1 + \cos^2\theta_Q$ angular distribution and presents upper limits on the number of events and on $R_Q(q\bar{q})$ for $Q = 2/3$ and $1.0 < m_Q < 2.8 \text{ GeV/c}^2$ [15]. As in the inclusive analysis, only the integrated luminosity from c.m. energies of 5.2 GeV and below is used for the lowest mass interval ($1.0 < m_Q < 1.25 \text{ GeV/c}^2$). This is in order to minimize efficiency corrections due to m_T^2 resolution effects, but it also insures that all tracks deposit more than their minimum ionization.

This work was supported primarily by the Department of Energy, under contracts DE-AC03-76SF00515 and W-7405-ENG-48. Support for individuals came from the listed institutions plus DAAD Bonn and Ecole Polytechnique.

References

- [1] G. S. LaRue, W. M. Fairbank and A. F. Hebard, Phys. Rev. Lett. 38 (1977) 1011; G. S. LaRue, W. M. Fairbank and J. D. Phillips, Phys. Rev. Lett. 42 (1979) 142; W. M. Fairbank, Proc. XXth Inter. Conf. on High Energy Physics, Madison, Wisconsin (1980).
- [2] G. Bathow et al., Phys. Lett. 25B (1967) 163.
- [3] J. Foss et al., Phys. Lett. 25B (1967) 166.
- [4] E. Bellamy et al., Phys. Rev. 166 (1968) 1391.
- [5] R. Galik et al., Phys. Rev. D4 (1974) 1856.
- [6] W. Bartel et al., Z. Phys. C6 (1980) 295.
- [7] G. S. Abrams et al., Phys. Rev. Lett. 43 (1979) 477.
- [8] G. S. Abrams et al., Phys. Rev. Lett. 43 (1979) 481.
- [9] G. S. Abrams et al., Phys. Rev. Lett. 44 (1980) 10.
- [10] These minimum ionizing tracks represent the tail of the m_T^2 distribution of light particles, visible in figs. 1a and 1b, where either the momentum is overestimated for high momentum particles with poor momentum resolution, or where lower momentum particles have had their times mis-measured by the time-of-flight system. The fraction of tracks with $m_T^2 > 1.6 (\text{GeV}/c^2)^2$ is 0.9×10^{-5} per detected light particle.
- [11] Particles which are calculated to range out in the scintillator are treated differently. We assume a certain fraction of their total kinetic energy will then be detected in scintillation light.

This fraction is determined experimentally from the deuterons to be $63 \pm 2\%$.

- [12] P. V. Vavilov, Zh. Eksp. Teor. Fiz. 32 (1957) 320 [Sov. Phys. JETP 5 (1957) 749].
- [13] S. M. Seltzer and M. J. Berger, NAS-NRC Pub.No.1133 (1964) 187.
- [14] J. M. Paul, Nucl. Instrum. Meth. 96 (1971) 51.
- [15] Two-body kinematics can be used to further discriminate between $Q = 2/3$ and $Q = 1$ particles. Except as an independent check, this offers no improvement, however, on the limits presented here.

Table I. 90% C.L. Upper Limits for $e^+e^- \rightarrow q\bar{q}X$ and $Q = -2/3$.

m_Q	Events		Eff.	$\int \mathcal{L} dt$ above thresh.	$\sigma(q\bar{q}X)$	aver. $E_{c.m.}$	$R_Q(q\bar{q}X)$
	maximum observed	limit					
1.0 - 1.25	11	10.8	.47	14154	2.3	4.5	5.6×10^{-4}
1.25 - 1.9	5	6.5	.49	19891	1.0	5.2	3.0×10^{-4}
1.9 - 2.1	3	6.8	.49	18920	0.76	5.3	2.3×10^{-4}
2.1 - 2.6	1	3.9	.50	13778	0.56	6.0	2.3×10^{-4}
2.6 - 3.0	1	3.9	.50	5178	1.5	6.7	8.0×10^{-4}
GeV/c^2				nb^{-1}	pb	GeV	

Table II. 90% C.L. Upper Limits for $e^+e^- \rightarrow q\bar{q}$ and $Q = 2/3$.

m_Q	Events		Eff.	$\int \mathcal{L} dt$ above thresh.	$\sigma(q\bar{q})$	aver. $E_{c.m.}$	$R_Q(q\bar{q})$
	observed	limit					
1.0 - 1.25	0	2.3	.38	14154	0.51	4.5	1.2×10^{-4}
1.25 - 1.8	0	2.3	.46	19891	0.30	5.2	0.9×10^{-4}
1.8 - 2.0	0	2.3	.51	18920	0.28	5.3	0.8×10^{-4}
2.0 - 2.4	0	2.3	.53	13778	0.37	6.0	1.6×10^{-4}
2.4 - 2.8	0	2.3	.53	5178	1.0	6.7	5.2×10^{-4}
GeV/c^2				nb^{-1}	pb	GeV	

Figure Captions

Fig. 1. Mass spectrum m_T^2 of tracks with $m_T^2 > 1.6 \text{ (GeV/c}^2\text{)}^2$ for
(a) $Q > 0$ and (b) $Q < 0$.

Fig. 2. (a) The measured energy loss for positive and negative tracks with $m_T^2 > 1.6 \text{ (GeV/c}^2\text{)}^2$. (b) The ratio of the measured energy loss to the most probable energy loss calculated for $Q = 1$.

Fig. 3. Scatter plot of m_T^2 versus apparent momentum for $Q < 0$ data satisfying vertex requirement and dE/dx cut for $Q = -2/3$. Also indicated are expected regions for typical quark masses $M_Q = 1.25$ and 2.3 GeV/c^2 .

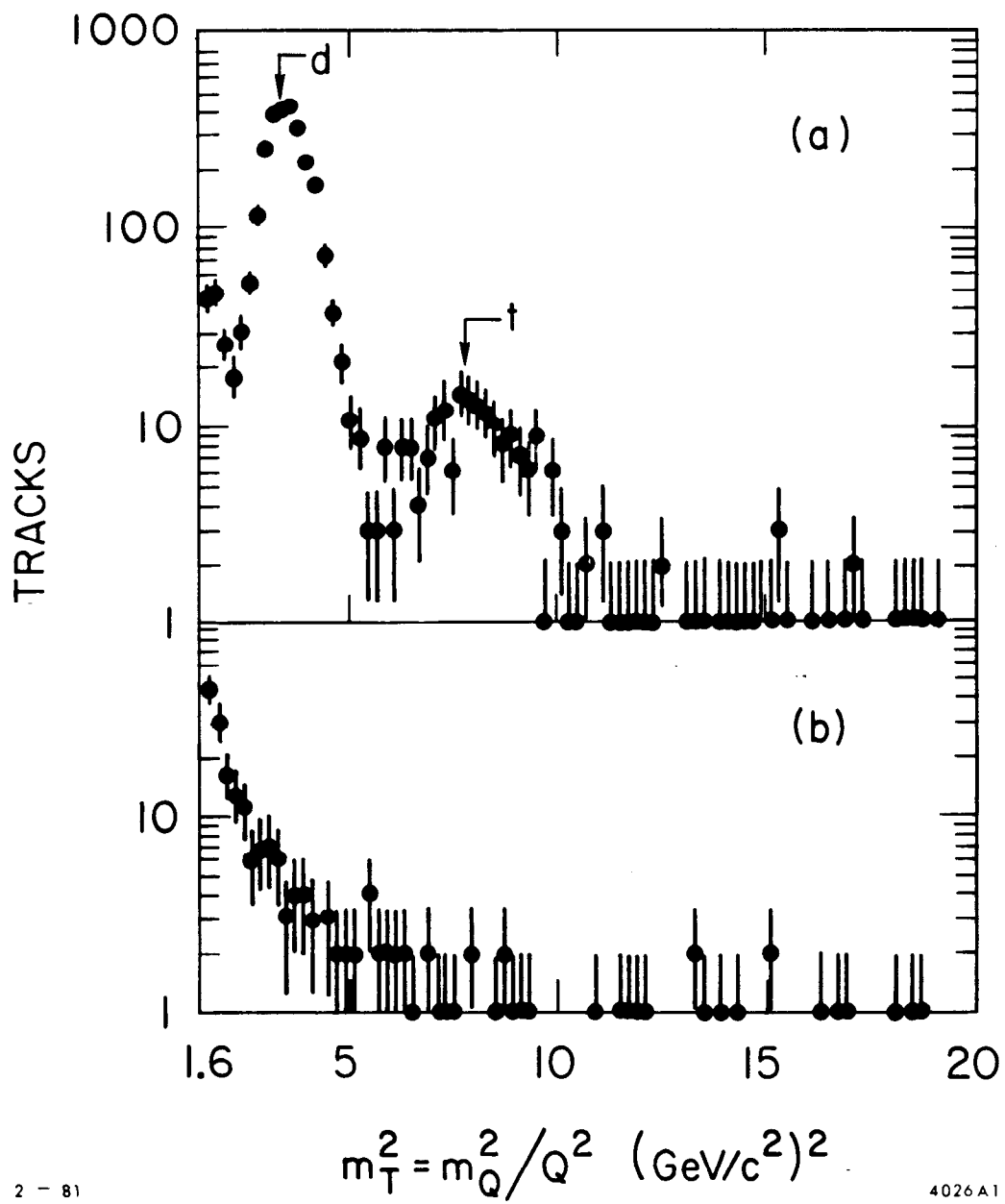
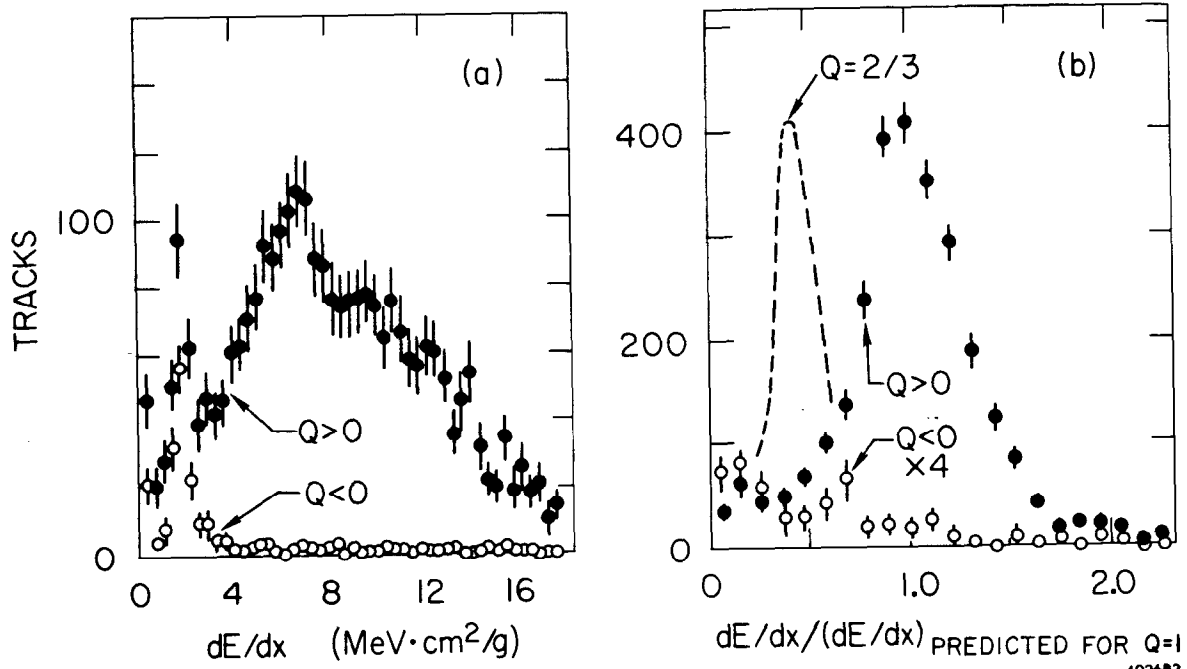


Fig. 1



2-81

Fig. 2

